

Available online at [www.sciencedirect.com](http://www.sciencedirect.com)

ScienceDirect

journal homepage: [www.elsevier.com/locate/AJPS](http://www.elsevier.com/locate/AJPS)

Original Research Paper

# Physicochemical properties of $\beta$ -cyclodextrin solutions and precipitates prepared from injectable vehicles <sup>☆</sup>

Sai Myo Thurein <sup>a,b</sup>, Nutdanai Lertsuphotvanit <sup>a</sup>,  
Thawatchai Phaechamud <sup>a,\*</sup>

<sup>a</sup> Department of Pharmaceutical Technology, Faculty of Pharmacy, Silpakorn University, Nakhon Pathom 73000, Thailand

<sup>b</sup> Department of Pharmacognosy, University of Pharmacy, Mandalay, Myanmar

## ARTICLE INFO

## Article history:

Received 28 November 2017

Accepted 26 February 2018

Available online 16 March 2018

## Keywords:

 $\beta$ -CyD solution

Precipitates

Dimethyl sulfoxide

N-methyl pyrrolidone

2-pyrrolidone

Matrix formation

## ABSTRACT

$\beta$ -Cyclodextrin ( $\beta$ -CyD) is cyclic oligosaccharide of a glucopyranose, containing a relatively hydrophobic central cavity and hydrophilic outer surface. However, the usefulness of  $\beta$ -CyD is limited owing to its low aqueous solubility whereas we found that its apparent high solubility was evident in some injectable solvents including 2-pyrrolidone (PYR), N-methyl pyrrolidone (NMP) and dimethyl sulfoxide (DMSO). Therefore, in the present study, the physicochemical properties of the 30–60% w/w  $\beta$ -CyD in PYR, NMP and DMSO were investigated such as viscosity, water resistant, matrix formation rate and syringeability. The higher the concentration of  $\beta$ -CyD resulted in the increased viscosity and the higher force and energy of syringeability.  $\beta$ -CyD in PYR gave the highest viscosity which contributed to the lowest syringeability while  $\beta$ -CyD in DMSO exhibited the highest syringeability. The  $\beta$ -CyD in DMSO and NMP exhibited the higher rate of matrix formation.  $\beta$ -CyD in PYR showed the highest water resistant for phase separation while  $\beta$ -CyD in NMP gave the faster de-mixing rate compared to that from PYR. The difference in physicochemical properties of  $\beta$ -CyD dried ppts studied by scanning electron microscope (SEM), differential scanning calorimetry (DSC), X-ray diffraction (XRD), Fourier-transform infrared spectroscopy (FT-IR) and thermogravimetric analysis (TGA) revealed that there was partial complexation of  $\beta$ -CyD with respective solvents. Both solution and precipitate characteristic properties will be useful for using  $\beta$ -CyD in further investigation as matrix material dissolved in the injectable vehicles as the *in situ* forming gel for periodontitis treatment.

© 2018 Shenyang Pharmaceutical University. Published by Elsevier B.V.

This is an open access article under the CC BY-NC-ND license.

<http://creativecommons.org/licenses/by-nc-nd/4.0/>

<sup>☆</sup> Peer review under responsibility of Shenyang Pharmaceutical University.

\* Corresponding author. Department of Pharmaceutical Technology, Faculty of Pharmacy, Silpakorn University, Nakhon Pathom 73000, Thailand. Tel.: 66 034 255800.

E-mail address: [thawatchaienator@gmail.com](mailto:thawatchaienator@gmail.com) (T. Phaechamud).

<https://doi.org/10.1016/j.ajps.2018.02.002>

1818-0876/© 2018 Shenyang Pharmaceutical University. Published by Elsevier B.V. This is an open access article under the CC BY-NC-ND license. (<http://creativecommons.org/licenses/by-nc-nd/4.0/>)

## 1. Introduction

The  $\beta$ -cyclodextrin ( $\beta$ -CyD) has a limited aqueous solubility [1,2] meaning that complexes resulting from interaction of lipophiles with this cyclodextrin exhibit the limited solubility resulting in precipitation of solid  $\beta$ -CyD complexes from water and other aqueous systems. Its low aqueous solubility character is interesting for using as a matrix former in solvent exchange-induced *in situ* forming gel. The main controlling step for the solvent exchange process is probably driven initially by water influx and onward by solvent efflux. This behavior is crucial for solvent-exchanged induced *in situ* forming gel [3]. In the periodontal pocket, the precipitation of polymer occurred after exposure the aqueous at injection site inducing the formation of a depot for consequent entrapping the drug with the controlled release manner [4]. Water is typically the solvent for inclusion complexation but this can be accomplished in a co-solvent system and in the presence of any non-aqueous solvents [5,6]. In the present study, the high concentrated  $\beta$ -CyD solutions were prepared using the injectable solvents including dimethyl sulfoxide (DMSO), *N*-methyl pyrrolidone (NMP) and 2-pyrrolidone (PYR). DMSO is miscible with water and organic solvents and it can be used as a polymer vehicle in *in situ* forming gel (ISG) and *in situ* forming microparticles (ISM) [7]. NMP is used as the organic solvent because of its solvating ability. Interestingly, a polar disubstituted cyclic amide group in NMP molecules has responsible for its interaction with water molecules for their complete miscibility. It acts as co-solvent owing to presence of the non-polar carbons of NMP which weakens the hydrogen-bonded structure of water [3]. It has been used in parenteral and oral dosage forms with thermally stable, biocompatible and biodegradable properties [8,9]. It is also used as an acceptable solvent which the solubility of NMP is similar to that of ethanol and DMSO [9,10]. NMP is used as solvent of Atridox<sup>®</sup> gel for delivering antimicrobial drug for periodontitis treatment. PYR is miscible with a wide variety of other solvents; therefore, it is used as a plasticizer and polymer solvent of *in situ* forming gel system [11] and ISM [12]. The objective of the present study is to investigate physicochemical properties of  $\beta$ -CyD solutions in DMSO, NMP and PYR which have not been reported before. Moreover, the  $\beta$ -CyD precipitates obtained from these solvents were characterized. These obtained data will be useful for applying the concentrated  $\beta$ -CyD solution in these injectable solvents as the *in situ* forming gel as delivery system to deliver the active compounds for periodontitis treatment.

## 2. Materials and methods

### 2.1. Materials

$\beta$ -CyD (lot no. 70P360) was kindly supported by Pharmanueva Co., Ltd., Bangkok, Thailand. NMP (lot no. A0251390, Fluka, New Jersey, USA), DMSO (lot no. 453035, Fluka, Switzerland) and PYR (lot no. BCBF5715V, Fluka, Germany) were used as the solvents for  $\beta$ -CyD. Potassium bromide (KBr) (spectrograde) was purchased from Fisher Scientific UK limited, UK and phosphoric acid (Merck KGaA, Darmstadt, Germany), potassium di-

hydrogen phosphate (KH<sub>2</sub>PO<sub>4</sub>) (ARgrade, lot no. P5104-1-1000, QREC Chemical CO, LTD, Chonburi, Thailand) were used as received.

### 2.2. Preparation of $\beta$ -CyD solutions

The 30%–60% (w/w)  $\beta$ -CyD solutions were prepared in NMP, DMSO and PYR by stirring until the clear solutions were obtained.

#### 2.2.1. Preparation of $\beta$ -CyD precipitates

The 20 g of 30% (w/w)  $\beta$ -CyD solution were titrated with distilled water until the initial phase separation was evident with precipitate formation. Then the amount of distilled water was continued to add to cause no further apparent precipitation. Then, the obtained precipitate was filtered and washed with cool distilled water several times to eliminate the solvent from precipitate and was dried in hot air oven at 60 °C for 2 d and kept in desiccator containing dried desiccant before test.

### 2.3. Evaluations

#### 2.3.1. Characterization of $\beta$ -CyD solutions prepared from three solvents

**2.3.1.1. Gel appearance, density and pH measurement** The appearance of the prepared formulations was examined visually, and the pH values of  $\beta$ -CD solutions were measured using a pH meter (Ultra 24 Basic UB-10, Denver Instrument, Bohemia, New York) ( $n = 3$ ). All samples were compared with pure solvents and distilled water. In addition, both pure solvents and  $\beta$ -CyD solutions were investigated for the density using pycnometer (Densito 30PX, Mettler Toledo Thailand Ltd, Portable-Lab TM) ( $n = 3$ ).

**2.3.1.2. Apparent viscosity** The appearance viscosity and rheology of the prepared  $\beta$ -CyD solutions were investigated at 25 °C using Brookfield DV-III Ultra programmable rheometer (Brookfield Engineering Laboratories, Inc., USA) ( $n = 3$ ). The apparent viscosity of pure solvents (DMSO, NMP and PYR) was determined.

**2.3.1.3. Measurement of water resistance** In order to determine the resistance of  $\beta$ -CyD solutions for inducing phase separation with water, the titration method with distilled water was used. The 20 g of 30% (w/w)  $\beta$ -CyD solutions in erlenmeyer flask were titrated with distilled water until the initial phase separation was evident. The amount of used water was recorded and expressed as the percentage to indicate the water resistance ( $n = 3$ ).

**2.3.1.4. Matrix formation** The observation of  $\beta$ -CyD matrix formation due to water diffusion into formulations was studied by filling each 150  $\mu$ l  $\beta$ -CyD solutions into the well with diameter of 6 mm of the 0.6% agarose gel containing PBS pH 6.8 which mimic artificial periodontal pocket [13]. When water diffused into the sample, the apparent system was changed from transparent to opaque insoluble  $\beta$ -CyD matrix. The distance of matrix formation (opaque front) with time

was recorded under a stereo microscope (Motic SMZ-171 Series). The rate of matrix formation into  $\beta$ -CyD solutions was correlated as opaque distance and time as Eq. (1):

$$\text{Rate of matrix formation} = \frac{\text{Distance of opaque front (mm)}}{\text{time (min)}} \quad (1)$$

**2.3.1.5. Solvent diffusion** To determine the characteristic of solvent diffusion, the 0.6% agarose gel containing PBS pH 6.8 with the cylindrical well (diameter of 6 mm) was filled with 150  $\mu$ l  $\beta$ -CyD solutions dyed with amaranth (0.1 g/10 ml). During solvent exchange, the change was captured with stereo microscope (Motic SMZ-171 Series) every 5 min for 30 min. The distance of amaranth diffusion front was measured in triplicate. The rate of solvent diffusion together with amaranth into agarose gels was correlated as Eq. (2).

$$\text{Rate of solvent diffusion into the gels} = \frac{\text{Distance of amaranth color front distance (mm)}}{\text{time (min)}} \quad (2)$$

**2.3.1.6. Syringeability test** For injectable formulation, syringeability of the systems is an important factor to be considered for the ease of administration to periodontal pocket. Syringeability test was determined by using texture analyzer (TA.XT plus, Stable Micro Systems, UK) in compression mode. The test sample was filled into 1 ml syringe with 27-gauge needle which is widely used in the dental field [14] and then this needle was clamped with stand. The upper probe of the texture analyzer moved downward until it comes into contact with the syringe barrel base. A constant speed of 1.0 mm/s and constant force of 0.1 N were applied. The distance required to expel the contents for a barrel length of 20 mm was measured and recorded. The work of injection was measured in triplicate at room temperature.

### 2.3.2. Characterization of dried $\beta$ -CyD precipitates

**2.3.2.1. Determination of morphology by inverted microscope** The ppts after dispersed in distilled water were dropped onto the slide and visually recorded their morphology every 10 s for 3 min under an inverted microscope (Nikon DXM 1200, Japan). Moreover, to observe the topography of systems, ppts were coated with gold prior to examination using scanning electron microscope (SEM) (Maxim 200 Camscan, Cambridge, England) at an accelerating voltage of 15 kVat magnifications of  $\times 200$ ,  $\times 500$ , and  $\times 2000$ .

**2.3.2.2. Determination of topography by scanning electron microscopy (SEM)** The topography of ppts was observed by SEM. The ppts were coated with gold prior to examination using scanning electron microscope (SEM) (Maxim 200 Camscan, Cambridge, England) at an accelerating voltage of 15 kVat magnifications of  $\times 200$ ,  $\times 500$ , and  $\times 2000$ .

**2.3.2.3. Morphology change under hot stage microscope (HSM)** Change of precipitate morphology was also studied using a hot stage microscope (HSM Mettler Toledo, model FP82HT, SNR 5130346892, Switzerland) at room temperature to 300 °C. The sample of 0.1 mg was placed on glass slides and heated at 5 °C/min.

**2.3.2.4. Melting point** A small quantity of powder was placed into a capillary tube and the tube was placed in the capillary melting apparatus (Melting point M-560, BUCHI, Switzerland) and the temperature was gradually increased automatically. The temperature at which powder started to melt and the temperature when all the powder completely melted were recorded ( $n = 3$ ).

**2.3.2.5. X-ray powder diffractometer** The X-ray diffraction (XRD) was performed upon the intact  $\beta$ -CyD and three  $\beta$ -CyD ppts. The ppts were filled into a glass sample holder with 0.2 mm depth and then loaded to an X-ray powder diffractometer (Miniflex II, Rigaku Corp. Tokyo, Japan). The  $\text{CuK}\alpha$  source ( $\lambda = 1.54 \text{ \AA}$ ) operated at 30 kV and 15 mA was used to record powder X-ray diffraction patterns in the  $2\theta$  range of 4°–60° at a step size of 2°/min.

**2.3.2.6. Differential scanning calorimetry (DSC)** The thermal properties of samples were determined using DSC (Pyris Sapphire DSC, Standard 115 V, Perkin Elmer instruments, Japan). The intact  $\beta$ -CyD and three  $\beta$ -CyD ppts were weighed accurately 5 mg into aluminum pan (PerkinElmer, Inc., MA, USA) and sealed and operated under dry nitrogen atmosphere which the measurement temperature was set at the ranges of 0 °C to 300 °C with heating rate of 10 °C/min.

**2.3.2.7. Thermogravimetric analysis (TGA) and differential thermogravimetric analysis (DTGA)** Thermal properties of intact  $\beta$ -CyD and three  $\beta$ -CyD ppts were determined using the thermal gravimetric analysis (TGA) (Pyris TGA, PerkinElmer, USA) The 15-mg intact  $\beta$ -CyD and three  $\beta$ -CyD precipitates were placed on an aluminum pan, and heated from 30 °C to 600 °C at 10 °C/min. The weight differences were recorded, and the percent weight loss was calculated. Then the differential thermogravimetric analysis (DTGA) was also calculated.

**2.3.2.8. Fourier-transform infrared (FT-IR) spectroscopy** The FT-IR spectra of the intact  $\beta$ -CyD and  $\beta$ -CyD ppts were recorded using KBr method using FT-IR spectrophotometer (FT/IR-4100, JASCO International Co., Ltd., Tokyo, Japan). Approximately 2 mg each sample was mixed and ground with 100 mg KBr before compressed into pellet using KBr die kit. The test was performed with the wave number ranges of 400–4000  $\text{cm}^{-1}$  with 32 scans at 4  $\text{cm}^{-1}$  resolution.

### 2.3.3. Statistical analysis

For statistical analysis of the measurements, the one-way analysis of variance (ANOVA) followed by the least significant difference (LSD) post hoc test was performed using PSPP for Windows. The significance level was set at  $P < 0.05$ .

## 3. Results and discussions

### 3.1. Characterization of $\beta$ -CyD solutions prepared from three solvents

#### 3.1.1. The gel appearance, density and pH measurement

The 30% (w/w)  $\beta$ -CyD was readily dissolved in all three injectable solvents. The 35%–40% (w/w)  $\beta$ -CyD was also dissolved in three different solvents but it was taken time about

**Table 1 – pH and density (mean  $\pm$  SD) for  $\beta$ -CyD solutions and its respective solvents (n = 3).**

$\beta$ -CyD conc. (% w/w)	NMP		DMSO		PYR	
	pH	Density (g/cm <sup>3</sup> )	pH	Density (g/cm <sup>3</sup> )	pH	Density (g/cm <sup>3</sup> )
0	12.284 $\pm$ 0.016	1.0287 $\pm$ 0.002	11.078 $\pm$ 0.385	1.092 $\pm$ 0.002	11.458 $\pm$ 0.01	1.106 $\pm$ 0.000
30	7.286 $\pm$ 0.001	1.141 $\pm$ 0.000	10.443 $\pm$ 0.003	1.192 $\pm$ 0.004	8.9 $\pm$ 0.298	1.195 $\pm$ 0.001
35	8.234 $\pm$ 0.006	1.159 $\pm$ 0.001	9.697 $\pm$ 0.002	1.210 $\pm$ 0.002	8.583 $\pm$ 0.012	1.213 $\pm$ 0.001
40	8.632 $\pm$ 0.002	1.294 $\pm$ 0.000	9.667 $\pm$ 0.003	1.227 $\pm$ 0.001	8.173 $\pm$ 0.011	1.812 $\pm$ 0.000
45	ND	ND	9.763 $\pm$ 0.004	1.236 $\pm$ 0.000	ND	ND
50	ND	ND	9.748 $\pm$ 0.004	1.255 $\pm$ 0.000	ND	ND
55	ND	ND	9.726 $\pm$ 0.004	1.265 $\pm$ 0.000	ND	ND
60	ND	ND	8.973 $\pm$ 0.03	1.296 $\pm$ 0.000	ND	ND

ND = not determined.

2 h to be completely dissolved. The rather clear solutions were obtained for 45% (w/w)  $\beta$ -CyD in NMP and PYR. The 45%–60% (w/w)  $\beta$ -CyD solutions required heating at temperature of 150 °C and stirring process to obtain the clear solution in DMSO which they were still clear solution after cooling down at room temperature.

PYR and its  $\beta$ -CD solutions showed the highest density and that of DMSO and its systems were slightly lower. NMP and its related solutions gave the lowest density among three solvents. The more the concentration of intact  $\beta$ -CD, the more increased density of the solution were attained (Table 1). The high density of PYR related with its high viscosity and could affect the diffusion property of these solvent. In addition the higher density of the developed solutions than water indicated that they could transform into matrix-like after exposure an aqueous environment and could deposit at bottom of target site such as periodontal pocket properly.

The pH of NMP was highest and followed by PYR and DMSO, respectively (Table 1). The increased amount of  $\beta$ -CD in the solution containing DMSO gradually decreased the pH of solution. However, the prominent reduction in pH was observed in the  $\beta$ -CD solution containing NMP and PYR. This may be due to the hydrogen formation of  $\beta$ -CD with lone pair electrons in NMP and PYR which led to the increase in acidity. But the steric hindrance effect of NMP caused less acidic than PYR [15].

### 3.1.2. Apparent viscosity

Viscosity, as an internal property of a fluid, offers the resistance to flow affecting abundant properties of *in situ* forming systems, especially the character of solvent exchange and diffusion rate [16]. PYR exhibited higher apparent viscosity than NMP and DMSO, respectively, and they were accounted for 10.61  $\pm$  0.22, 8.01  $\pm$  0.06 and 0.82  $\pm$  0.04 cPs, respectively. This result corresponded with the density value as mentioned previously. The apparent viscosity of solvents was noticeably increased when  $\beta$ -CyD was added. This proved the strong interaction of respective solvent with  $\beta$ -CyD molecule. Among them, the 40% (w/w)  $\beta$ -CyD solution in PYR showed the highest viscosity (99.67  $\pm$  0.12 cPs) due to apparent higher viscosity of solvent itself while that of NMP and DMSO exhibited lower viscosity of 45.7  $\pm$  8.6 cPs and 29.4  $\pm$  8.40 cPs, respectively. The trend of apparent viscosity of

$\beta$ -CyD solutions using different solvents were PYR  $\gg$  NMP  $>$  DMSO.

In this study, the curves moved to a higher shear stress value when concentration of  $\beta$ -CyD was increased in all solutions signifying the compact structure of the gels [17]. By comparison, the  $\beta$ -CyD solution in PYR showed the highest shear stress which was followed by that dissolved in NMP and DMSO, respectively. All the  $\beta$ -CyD solutions showed the Newtonian flow (Fig. 1). Typically, for ease of injection, the optimal rheological behavior of the *in situ* forming gel should be a Newtonian or pseudoplastic flow [18].

### 3.1.3. Water resistance of $\beta$ -CyD solutions

The titration with distilled water was used to determine the resistance for phase separation of  $\beta$ -CyD solutions. The different pairs of  $\beta$ -CyD-solvent exhibited different phase separation behavior or the precipitation pattern. The  $\beta$ -CyD in PYR showed the highest tolerance for phase separation while  $\beta$ -CyD in NMP gave the faster de-mixing rate compared to that from PYR. PYR has less affinity with water [11] and the system containing PYR was more viscous [19] which retarded the diffusion rate of water into the  $\beta$ -CyD solution. Thus, the amount of water used for phase separation of  $\beta$ -CyD containing PYR was higher and the amount of water used for phase separation of 30%  $\beta$ -CyD solution in PYR was 258.34%  $\pm$  2.89% (w/w). The polar nature of the solvents has high affinity with water as the like dissolve like theory. The polarity of DMSO was higher than 2-pyrrolidone [20,21]. Owing to the high affinity with water and lower viscosity than that of PYR, the de-mixing rate of  $\beta$ -CyD from DMSO was more rapid than PYR. The amount of water used for phase separation of  $\beta$ -CyD solution containing DMSO was 180.00%  $\pm$  7.55% (w/w). The polar disubstituted cyclic amide group of NMP molecule can interact with water molecules causing the complete miscibility [3]. In addition, the less viscous behavior of NMP allowed the water molecule to penetrate into  $\beta$ -CyD solution easily and rapidly. Hence, the  $\beta$ -CyD solution containing NMP showed the fastest de-mixing rate with the small volume of water (74.17%  $\pm$  1.04%, w/w).

### 3.1.4. Matrix formation and solvent diffusion

The solvent exchange process was probably driven initially by water influx and onward by solvent efflux. This behavior is crucial for solvent-exchanged induced *in situ* forming gel

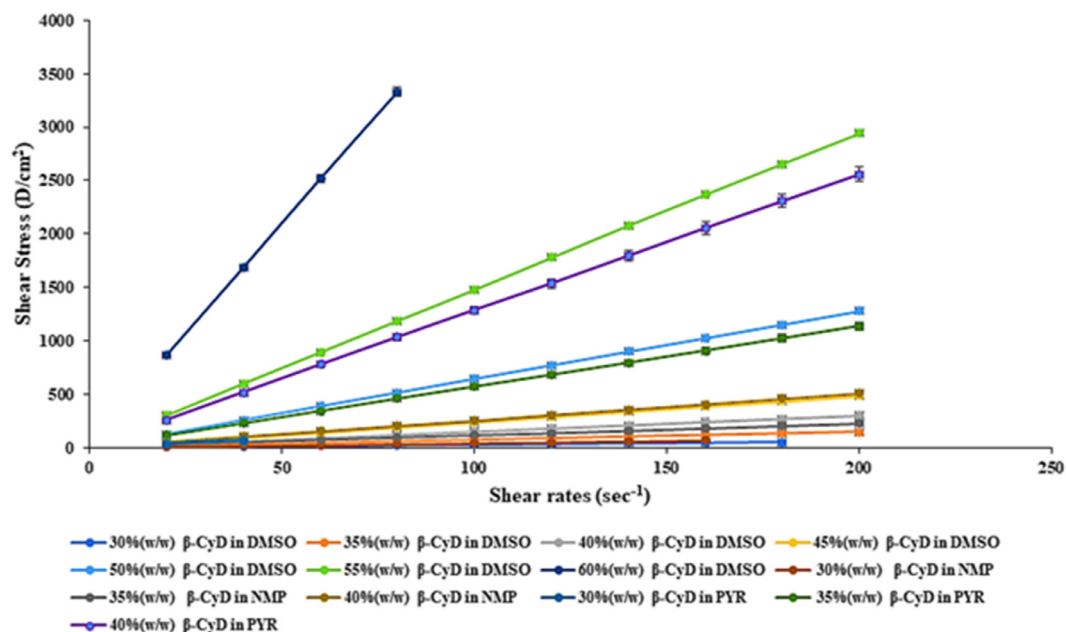


Fig. 1 – Rheological properties of  $\beta$ -CyD solutions.

or ISM to transform from solution or emulsion, respectively, into gel or microparticle [3]. The rate limiting step of structure change into gel formation or solid matrix was the diffusion rate of aqueous into the  $\beta$ -CyD solution [18]. Therefore, the effect of solvents on diffusion rate and the  $\beta$ -CyD matrix formation were studied. When the PBS diffused into the  $\beta$ -CyD solution, the solvent exchange process happened, and the solvent diffused into the surrounding aqueous environment. Consequently, the water diffused into the  $\beta$ -CyD solution and opaque-ring was occurred as phase separation zone which represented the process of matrix formation from outer area to inner area which the enlargement of this band was increased by time. Owing to the strong water miscibility of NMP, the diffusion rate of water into  $\beta$ -CyD solution and transformation rate into matrix was rapid (Fig. 2A and B). The opaque band of  $\beta$ -CyD solution using PYR as solvent was small because of the high viscosity of solvent itself. The DMSO has a high affinity with water [22]. In addition, the  $\beta$ -CyD solution containing DMSO as solvent promoted a rapid phase inversion than that of the PYR owing to its less viscous nature [23]. However, the transformed solid-like matrix behaved like a thicker barrier with time for the aqueous penetration into inner system. Thus, the diffusion path was lengthened, and the penetration of water was gradually slower with time.

In ISG system, the solvent typically diffuses into the surrounding aqueous environment and water diffuses into the polymer matrix and then the polymer precipitates and thereafter the formation of a solid-like matrix is occurred [24]. Thus, the amaranth front movement was used to indicate the solvent diffusion. The diffusion of solvent together with amaranth as red front into the surrounding environment was investigated under stereomicroscope. The movement of solvent front was occurred after 5 min (Fig. 2C). Owing to the high affinity of water and least viscosity nature of NMP, the

rapid exchange of solvent with water was observed. This led to the lowest distance of solvent front movement whereas the more viscous DMSO created the slower diffusion of water and matrix formation rate. This allowed the movement of solvent front to be longer. Thus, the distance of solvent front of DMSO was higher than that of the NMP. The highest solvent front was occurred in the  $\beta$ -CD solution containing PYR.

### 3.1.5. Syringeability test

The present study indicates that the force of syringeability between  $\beta$ -CyD solutions was statistically different. The increasing  $\beta$ -CyD content increased the work required for expulsion indicating lower syringeability. Fig. 3 shows the work force for syringeability of the  $\beta$ -CyD solutions and pure solvents. Higher concentration of  $\beta$ -CyD in NMP at 45% (w/w) and that of PYR of >40% (w/w) could not be expelled through the 27-gauge needle. By comparison, PYR exhibited particularly lower syringeability than others owing to the highest viscosity of PYR. The solvent affinity to the polymer could affect the syringeability of the ISG. A good solvent is dominant the polymer-solvent interaction over the polymer-polymer which leads to lowering the viscosity [11]. Typically, the preparations with the applied force lower than 50N were acceptable as injectable dosage forms [25]. Among three solvents, DMSO could solubilize the high amount  $\beta$ -CyD and gave the higher syringeability indicating the ease of administration of *in situ* forming system by injection.

## 3.2. Characterization of $\beta$ -CyD dried ppts

### 3.2.1. Morphology under inverted microscope

Intact  $\beta$ -CyD exhibited the definite rhombic dodecahedral large crystals as previously reported [26]. The ppt obtained from DMSO exhibited the small irregular structure which was

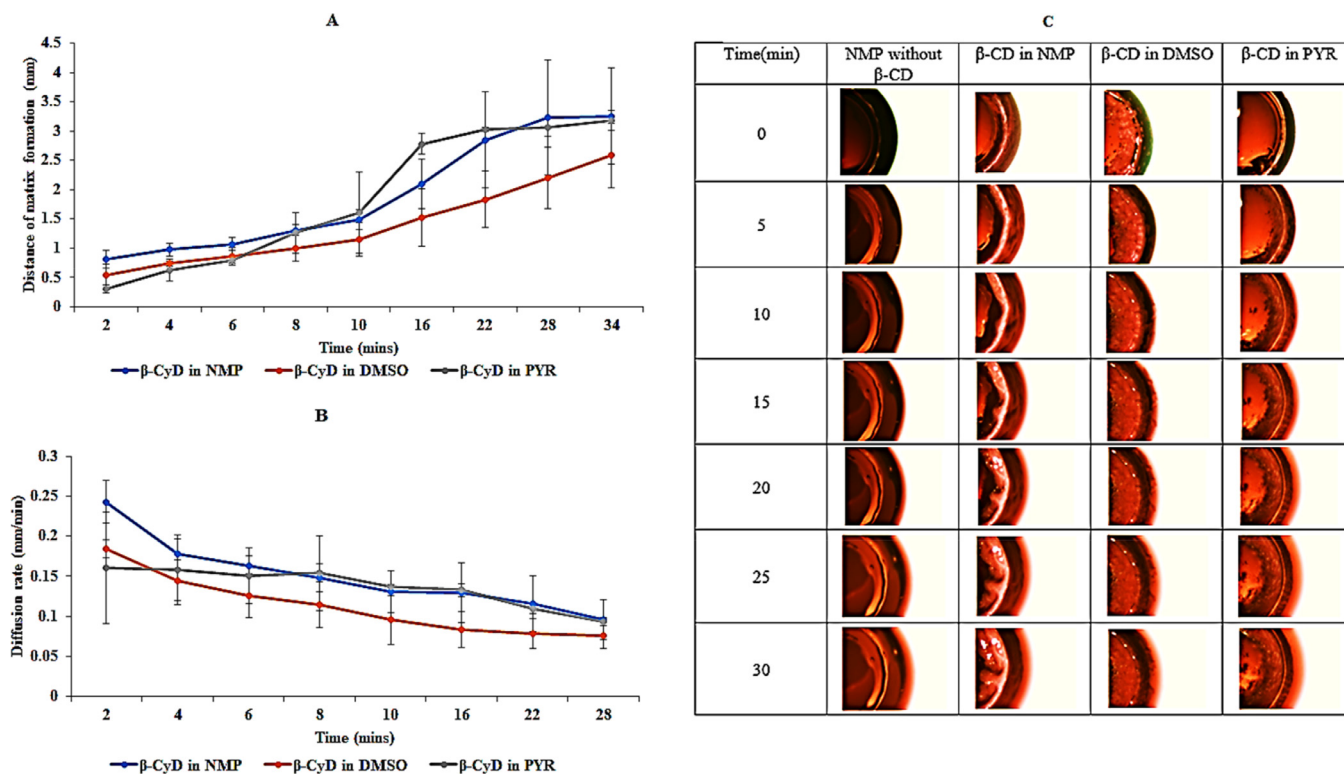


Fig. 2 – Distance of matrix formation (A) and rate of matrix formation (B) (n = 3); (C) visual image of solvent diffusion of systems prepared with different solvents containing amaranth as a colorant.

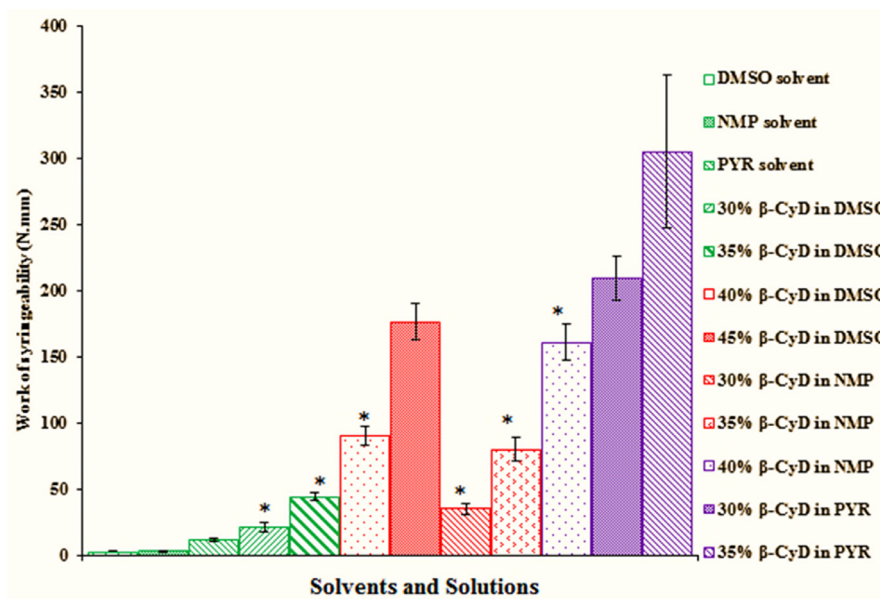
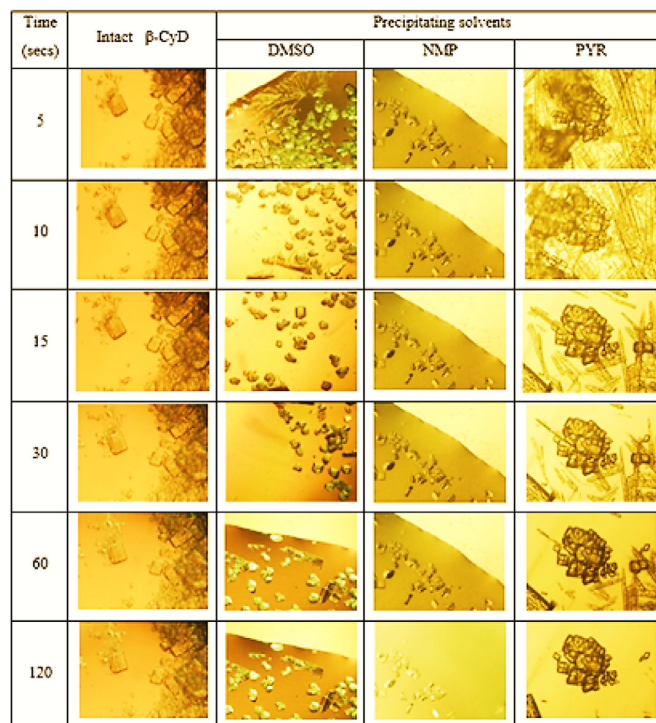


Fig. 3 – Syringeability of pure solvents and  $\beta$ -CyD solution (n = 3), \*P < 0.05.

deformed with time (Fig. 4). The smaller particle size of  $\beta$ -CyD ppt obtained from DMSO was due to the solubility of  $\beta$ -CyD in DMSO which was proved by the higher amount of water used to precipitate the  $\beta$ -CyD in water resistant study. However, some well-defined structure was still occurred in DMSO ppt which indicated that  $\beta$ -CyD might partially complexed

with DMSO. The substantially large and nearly planar non-polar region of NMP may lead to hydrophobic interaction between NMP and  $\beta$ -CyD molecule to form a complex [3]. On the other hand, the ppt obtained from PYR resembled in bundle of rhombic dodecahedral crystals which look likes dendrites and it might be due to the aggregation formation between  $\beta$ -CyD



**Fig. 4 – Morphology of dried  $\beta$ -CyD ppts after dispersed in distilled water under inverted microscope (10 $\times$ ).**

and PYR (Fig. 4). Therefore, the obtained  $\beta$ -CyD ppts exhibited the quite different morphology from that of the intact  $\beta$ -CyD.

### 3.2.2. Morphology by SEM

The large well-defined flake-type crystalline particles were found in the intact  $\beta$ -CyD (Fig. 5). The morphology of ppts from DMSO showed the well-defined surface similar to the intact  $\beta$ -CyD and this unchanged crystal particles proved no interaction between DMSO and  $\beta$ -CyD because the strong interaction between compound and CDs caused no more possible for differentiation of the crystals of both components [27]. In addition, the guest/host inclusion complexes can increase the tendency of  $\beta$ -CyD molecules to form aggregates [28]. The agglomerate aggregated on flake type crystalline particles was observed in NMP ppt while the rod-like aggregates were observed in PYR ppt whereas the change in the morphology of intact  $\beta$ -CyD was observed. This change in morphology of ppts might be the indicative partial complexation or aggregation of  $\beta$ -CyD with NMP and PYR.

### 3.2.3. Morphology from hot stage microscopy (HSM)

The HSM photomicrograph revealed that the crystalline structure of intact  $\beta$ -CyD did not alter any modification (Fig. 6). For  $\beta$ -CyD ppts from NMP and DMSO, their crystalline structures were observed at low temperature. The behavior of ppt obtained from DMSO showed similar characteristic to intact  $\beta$ -CyD signifying the  $\beta$ -CyD partially complexed with DMSO. But heating to higher temperature (290 °C), the partial melting of crystals was occurred. In the case of the  $\beta$ -CyD ppt from DMSO, the small and large vesicles were also observed. The melting of the  $\beta$ -CyD ppt crystal from PYR was observed

even at low temperature. Thus, HSM proved the evidence of the changes for the character of the intact  $\beta$ -CyD when it dissolved in solvents with the partial complexation with solvents.

### 3.2.4. Melting point of $\beta$ -CyD precipitates

Although there is no definite melting point, CyDs have begun to decompose from about 200 °C and above [29]. In the present study, the melting point of intact  $\beta$ -CyD was occurred within the range of 267.5–269.3 °C. Comparison among  $\beta$ -CyD precipitates, the  $\beta$ -CyD in NMP gave the highest melting point of 296.8 °C which was followed by  $\beta$ -CyD in PYR and  $\beta$ -CyD in DMSO. The value of their melting points was accounted for 293.0 °C for PYR and 283.6 °C for DMSO respectively. The new arrangement of crystalline structure of  $\beta$ -CyD precipitated from solvents as seen from above SEM results together with complexation between  $\beta$ -CyD and respective solvent could occur because the melting point of  $\beta$ -CyD precipitates was higher than that of intact  $\beta$ -CyD. The inclusion complexation could increase the thermal stability [27].

### 3.2.5. X-ray powder diffraction

Diffraction patterns of intact  $\beta$ -CyD exhibited a series of thin and intense lines corresponding to its crystallinity shown in Fig. 7A. When the respective solvent was introduced into the cavities of  $\beta$ -CyD during the formation of inclusion complex, the similar diffraction with intact  $\beta$ -CyD might be obtained [30]. The similar diffraction patterns with low intensities were observed in  $\beta$ -CyD ppts. Moreover, the intensity of sharp maximum peak presented in intact  $\beta$ -CyD was reduced in that of DMSO and PYR ppts indicating the partial

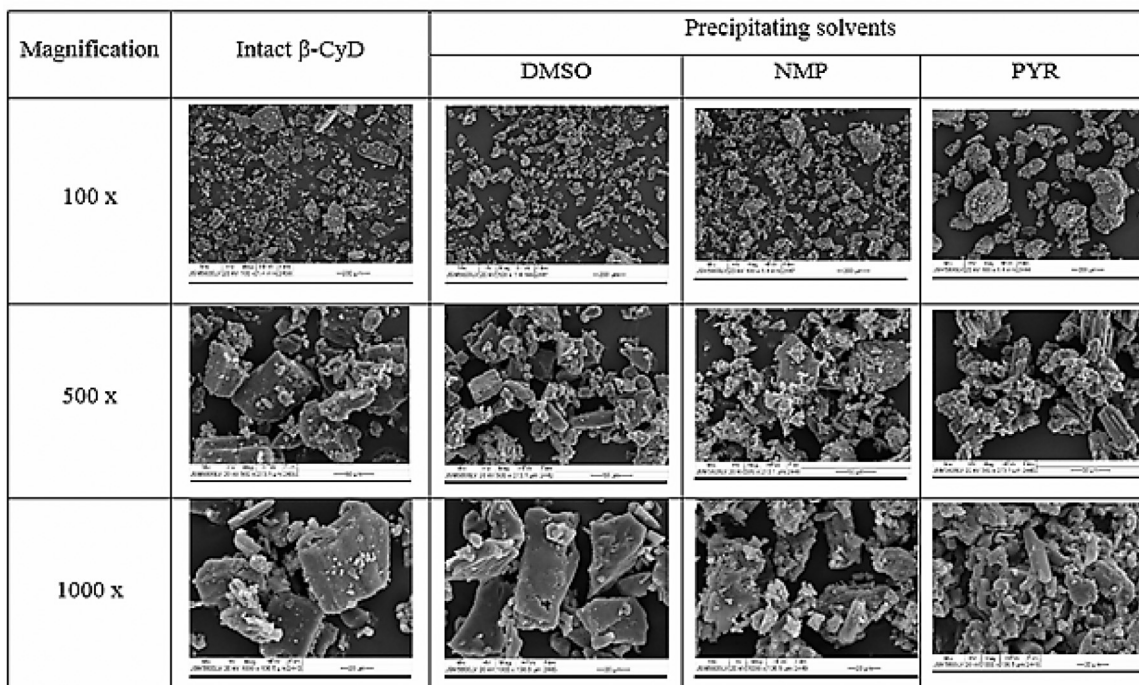


Fig. 5 – SEM photomicrographs of intact  $\beta$ -CyD and  $\beta$ -CyD precipitates from different solvents.

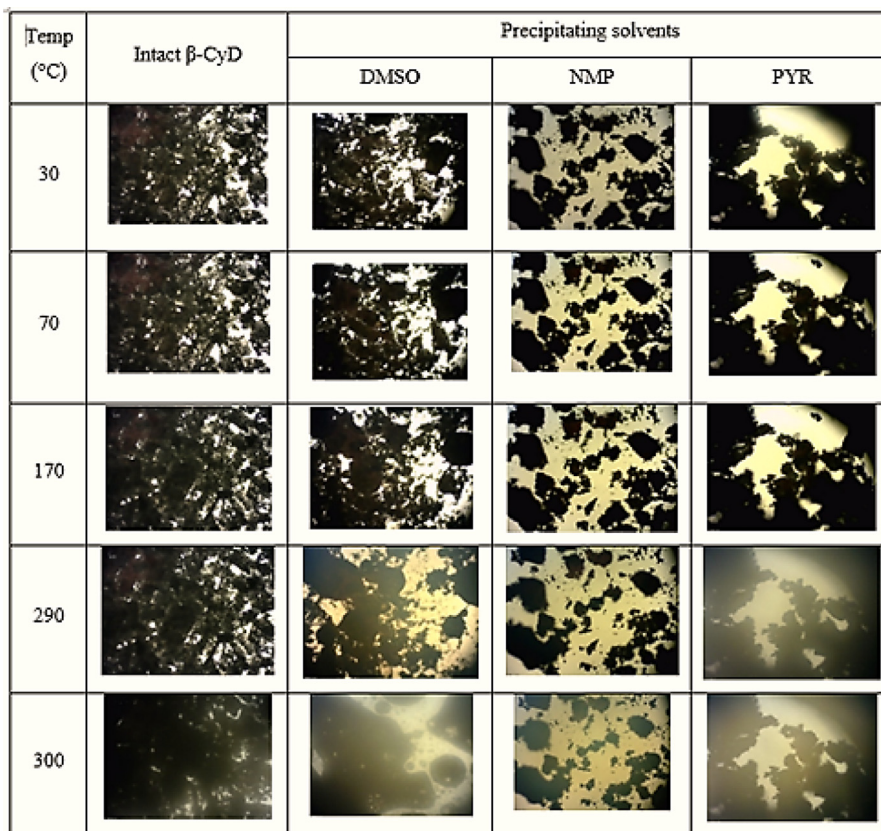


Fig. 6 – Morphology of intact  $\beta$ -CyD and  $\beta$ -CyD precipitates from different solvents under HSM (40x).

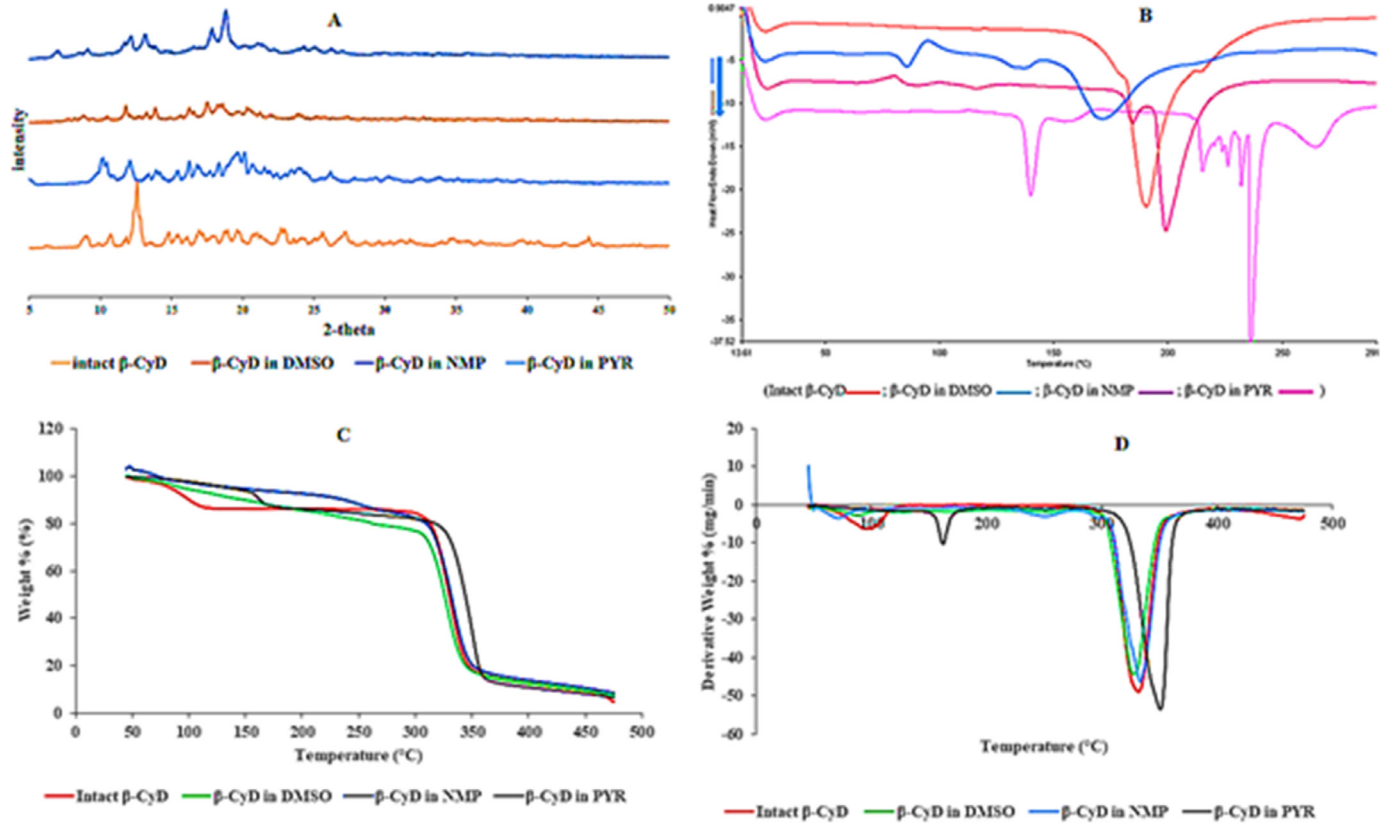
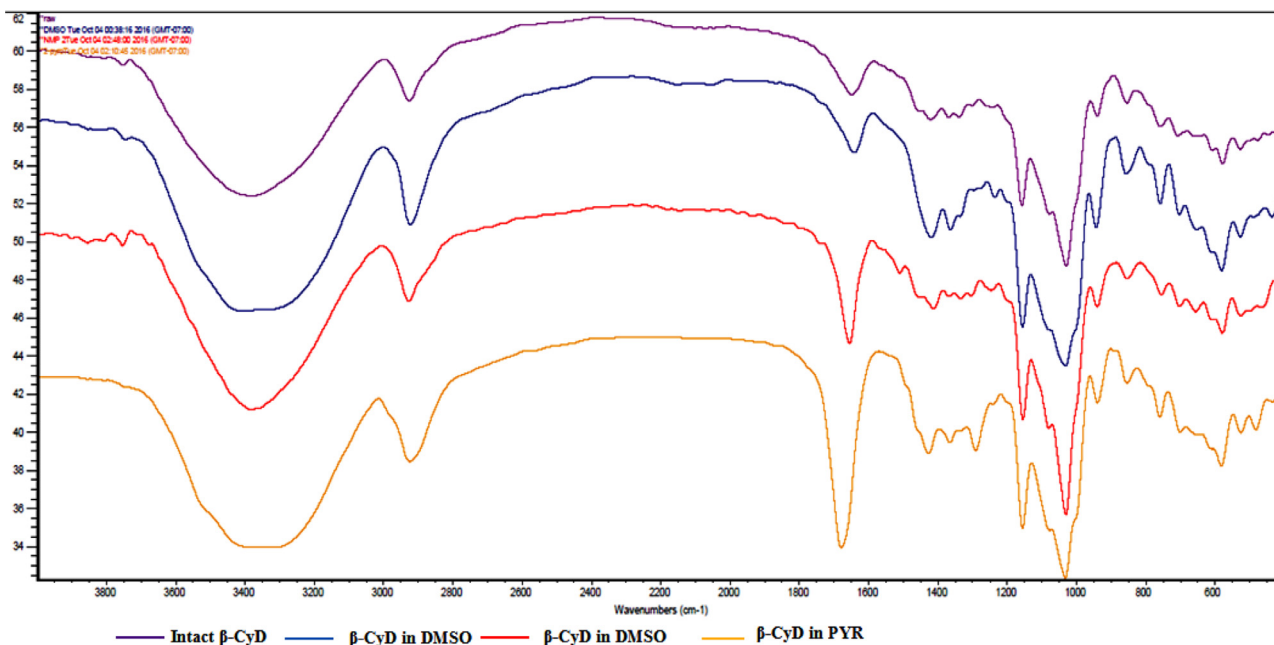


Fig. 7 – (A) XRD diffractograms; (B) DSC thermograms; (C) TGA curves and (D) DTGA curve of intact  $\beta$ -CyD and  $\beta$ -CyD ppt prepared from different solvents (DMSO, NMP and PYR).



**Fig. 8 – FT-IR spectra of intact  $\beta$ -CyD and  $\beta$ -CyD precipitates prepared from different solvents.**

complexation behavior. The partial complexation between  $\beta$ -CyD and PYR might be due to the hydrophobic part of solvent molecules incorporated into the  $\beta$ -CyD cavity [3] while the partial complexation between  $\beta$ -CyD and DMSO might be the result of the of hydrogen bond formation to an oxygen atom of DMSO and hydroxyl group of  $\beta$ -CyD [22]. The sharp maximum peak of intact  $\beta$ -CyD was not occurred in ppt obtained from NMP and the peak was dispersed in this ppt. Therefore, the different and lower intensities may be indicative of partial complexation.

### 3.2.6. Differential scanning calorimetry (DSC)

The intact  $\beta$ -CyD exhibited only a broad endothermic peak at 180 °C and no peaks were observed below 150 °C. The peak of DMSO ppt was shifted to lower temperature and the residual presence of the drug melting peak is the indication of the existence of free drug molecules which suggested that there was no or not complete inclusion complexation [31] which was in accordance with the SEM study. The  $\beta$ -CyD ppt derived from NMP exhibited a broad endothermic peak which was similar to intact  $\beta$ -CyD, but the peak was shifted to higher temperature. The PYR ppt gave the residual peak of the pure solvent at 140 °C and the sharp endothermic peak of  $\beta$ -CyD was shifted to 240 °C. The results are shown in Fig. 7B. The solid-states interactions caused the energy activation for the decomposition of  $\beta$ -CyD which could lead to the change in the temperature peak of the  $\beta$ -CyD dehydration band [32]. Typically, the increased decomposition temperature might be assumed as the increased thermal stability of the inclusion complex [33]. Therefore, the DSC thermogram of  $\beta$ -CyD ppts indicated a sign of partial inclusion complex of  $\beta$ -CyD with respective solvents.

### 3.2.7. Thermogravimetric analysis (TGA) and derivative of thermogravimetric analysis (DTGA)

The thermogravimetric analysis (TGA) was carried out to identify the changes in weight percent with respect to temperature

change. TGA reveals that intact  $\beta$ -CyD exhibited two stages of weight loss (Fig. 7C and D). Loss of water molecules from intact  $\beta$ -CyD cavity occurred at 76 °C in the first stage. The degradation temperature of cyclodextrin has been reported at about 300 °C [34], which the weight loss related to the decomposition of intact  $\beta$ -CyD was occurred at 305 °C. The flat curve of TG was observed between 120 °C and 280 °C and no mass loss was detected [35]. For  $\beta$ -CyD ppt derived from DMSO, the first stage of loss of water molecule occurred in intact  $\beta$ -CyD was disappeared and it exhibited only one mass loss at 299 °C. This different weight loss pattern occurred in ppt derived from DMSO was the indicative of the partial complexation behavior. First weight loss for  $\beta$ -CyD ppt derived from NMP started at 73 °C which was similar to the water loss of intact  $\beta$ -CyD. The second mass loss for  $\beta$ -CyD ppt derived from NMP was decreased to 225 °C which indicates the decrease in thermal stability of  $\beta$ -CyD ppt [36]. In case of the mass loss for ppt derived from PYR, it gave two stages of weight loss as occurred in intact  $\beta$ -CyD except the water loss temperature was increased to 157 °C and the second decomposition temperature was increased above 310 °C. The residual weight of  $\beta$ -CyD ppt above 300 °C after thermal decomposition exhibited similar weight to that of the intact  $\beta$ -CyD which indicates the partial incorporation of  $\beta$ -CyD in respective solvents. The TGA of pure solvents were studied and compared with that of the  $\beta$ -CyD ppts (data not shown). The TGA of the pure NMP and PYR revealed the weight loss between 90 °C and 200 °C while the complete weight loss of DMSO was occurred earlier than NMP and PYR which was happened below 100 °C. This may be due to the boiling point of DMSO which accounted for 189 °C [37]. As the boiling point of NMP was 202 °C [3] and that of PYR was 245 °C [38], there was no residual weight of pure solvents were observed above 250 °C. This observation was corresponded to the residual weight observed in  $\beta$ -CyD ppt above 300 °C which was the component of  $\beta$ -CyD; therefore, this thermal behavior

indicated the complexation of  $\beta$ -CyD with solvents. The two stages of weight loss were occurred in intact  $\beta$ -CyD and they were accounted for 10% and 50% weight loss at 100 °C and 325 °C, respectively. The two stages of %weight loss for ppt obtained from DMSO was less than that of intact  $\beta$ -CyD. The three stages of weight loss for ppt obtained from NMP were occurred and the temperature for first weight loss was less than that of the intact  $\beta$ -CyD. On the other hand, the prominent different weight loss pattern was obtained in ppt form PYR which the weight loss was more than 10% and 50% at 160 °C and 350 °C, respectively. This phenomenon indicates that the  $\beta$ -CyD ppts had changed the thermal degradation properties of intact  $\beta$ -CyD which proves that the morphology of the intact  $\beta$ -CyD was changed.

### 3.2.8. Fourier-transform infrared spectroscopy

FTIR spectrum of intact  $\beta$ -CyD and precipitates is shown in Fig. 8. The prominent peak of intact  $\beta$ -CyD in the region of 3000–3500  $\text{cm}^{-1}$  was due to O–H stretching vibration [39]. The vibration of –CH and –CH<sub>2</sub> groups was occurred in the 2800–3000  $\text{cm}^{-1}$  region [40]. The C=O group gave the strong absorption near 1820–1660  $\text{cm}^{-1}$ , C–O asymmetric stretching and OH bending were occurred in the range of 1200–1000  $\text{cm}^{-1}$ , respectively [39]. Almost similar peak at wave-number of the intact  $\beta$ -CyD was observed in the obtained ppts. However, overlapping of O–H and C–H group promoted in peak broadening of  $\beta$ -CyD ppts. Other corresponding peaks of O–H, C–H (bending), C=O, C–H (stretching) occurred in intact  $\beta$ -CyD were evident at the lower frequencies in ppts. Although the functional group of the intact  $\beta$ -CyD was not changed, strong intensities in the area between 1800  $\text{cm}^{-1}$  in PYR and NMP ppts proved the insertion of molecules into the electron rich cavity of  $\beta$ -CyD and it caused to increase the density of electron cloud, which led to the increase in frequency [41].

## 4. Conclusion

Owing to the highest viscosity of the solvent itself, the  $\beta$ -CyD solutions containing PYR as solvent exhibited the highest viscosity which was followed by the  $\beta$ -CyD solution prepared from DMSO and NMP, respectively. The  $\beta$ -CyD dissolved in NMP and DMSO exhibited the higher rate of solvent diffusion and solid matrix formation. In addition, the high concentrated  $\beta$ -CyD could be prepared in injectable solvents, especially in DMSO, with low viscosity and Newtonian flow.  $\beta$ -CyD in PYR exhibited the highest water resistance and its matrix formation was lower than that in DMSO and NMP. From DSC, TGA, X-ray diffraction and FT-IR data,  $\beta$ -CyD precipitates prepared from these solvents showed the complexation between  $\beta$ -CyD and solvent molecules. Therefore, these characteristic properties will be useful for further using  $\beta$ -CyD solutions as matrix former in the *in situ* forming gel for periodontitis treatment.

## Conflicts of interest

The authors declare that there is no conflicts of interest.

## Acknowledgments

The researchers are grateful to the Research and Development Institute, Silpakorn University. This research work was also facilitated by the Faculty of Pharmacy, Silpakorn University, Thailand.

## Supplementary materials

Supplementary material associated with this article can be found, in the online version, at [doi:10.1016/j.ajps.2018.02.002](https://doi.org/10.1016/j.ajps.2018.02.002).

## REFERENCES

- [1] Loftsson T, Brewster ME. Review article pharmaceutical applications of cyclodextrins: 1. Drug solubilization and stabilization. *J Pharm Sci* 1996;85(10):1017–25.
- [2] Magnúsdóttir A, Mátsson M, Loftsson T. Cyclodextrins. *J Incl Phenom Macroc Chem* 2002;44:213–18.
- [3] Sanghvi R, Narazaki R, Machatha SG, Yalkowsky SH. Solubility improvement of drugs using N-methyl pyrrolidone. *AAPS Pharm Sci Technol* 2008;9(2):366–76.
- [4] Phaechamud T, Mahadlek J. Solvent exchange-induced *in situ* forming gel comprising ethyl cellulose-antimicrobial drugs. *Int J Pharm* 2015;494:381–92.
- [5] Frömring KH, Szejtli J. Cyclodextrin. In: *Cyclodextrins in pharmacy*. Kluwer Academic Publishers; 1994. p. 1–81.
- [6] Del Valle EMM. Cyclodextrin and their uses: a review. *Process Biochem* 2004;39(9):1033–46.
- [7] Ahmed TA, Ibrahim HM, Samy AM, Kaseem A, Nutan MTH, Hussain MD. Biodegradable injectable *in situ* implants and microparticles for sustained release of Monyrllukast: *in vitro* release, pharmacokinetics, and stability. *AAPS Pharm Sci Technol* 2014;5(3):772–80.
- [8] Strickley RG. Solubilizing excipients in oral and injectable formulations. *Pharm Res* 2004;21(2):201–30.
- [9] Jouyban A, Fakhree MA, Shayanfar A. Review of pharmaceutical applications of N-methyl-2-pyrrolidone. *J Pharm Pharm Sci* 2010;13:524–35.
- [10] Hansen CM, Just L. Prediction of environmental stress cracking in plastics with Hansen solubility parameter. *Ind Eng Chem Res* 2001;40(1):21–5.
- [11] Parent M, Nouvel C, Koerber M, Sapin A, Maincent P, Boudier A. PLGA *in situ* implants formed by phase inversion: critical physicochemical parameters to modulate drug release. *J Control Release* 2013;172(1):292–304.
- [12] Kranz H, Brazeau GA, Napaporn J, Martin RL, Millard W, Bodmeier R. Myotoxicity studies of injectable biodegradable *in-situ* forming drug delivery systems. *Int J Pharm* 2001;212(1):11–18.
- [13] Do MP, Neut C, Delcourt E, Certo TS, Siepmann J, Siepmann F. *In situ* forming implants for periodontitis treatment with improved adhesive properties. *Eur J Pharm Biopharm* 2014;88:342–50.
- [14] Sato Y, Oba T, Watanabe N, Danjo K. Development of formulation device for periodontal disease. *Drug Dev Ind Pharm* 2012;38(1):32–9.
- [15] Le Questel JY, Laurence C, Lachkar A, Lachkar A, Helbert M, Berthelot M. Hydrogen-bond basicity of secondary and tertiary amides, carbamates, ureas and lactams. *J Chem Soc Perkin Trans 2* 1992;12:2091–4.

- [16] Phaechamud T, Praphanwittaya P, Laotaweesub K. Solvent effect on fluid characteristics of doxycycline hyclate-loaded bleached shellac *in situ*-forming gel and -microparticle formulations. *Int J Pharm Invest* 2017 In Press.
- [17] Priyanka M, Meenakshi B. Study of secnidazole-serratiopeptidase alginate/HPMC gels for periodontal delivery. *Int J Pharm Technol Res* 2011;3(3):1488–94.
- [18] Phaechamud T, Mahadlek J. Solvent exchange-induced *in situ* forming gel comprising ethylcellulose-antimicrobial drugs. *Int J Pharm* 2015;494(1):381–92.
- [19] Phaechamud T, Chanyaboonsub N, Setthajindalert O. Doxycycline hyclate-loaded bleached shellac *in situ* forming microparticle for intraperiodontal pocket local delivery. *Eur J Pharm Sci* 2016;93:360–70.
- [20] George J, Sastry NV. Densities, viscosities, speeds of sound, and relative permittivities for water + cyclicamides (2-pyrrolidinone, 1-methyl-2-pyrrolidinone, and 1-vinyl-2-pyrrolidinone) at different temperatures. *J Chem Eng Data* 2004;49:235–42.
- [21] Hollingsworth CA. Equilibrium and the rate laws. *J Chem Phys* 2004;20(10):921.
- [22] Shikata T, Takahashi R, Onji T, Satokawa Y, Harada A. Solvation and dynamic behavior of cyclodextrins in dimethyl sulfoxide solution. *J Phys Chem* 2006;110(37):18112–14.
- [23] Packhaeuser CB, Schnieders J, Oster CG, Kissel T. *In situ* forming parenteral drug delivery systems: an overview. *Eur J Pharm Biopharm* 2004;58:445–55.
- [24] Phaechamud T, Jantadee T, Mahadlek J, Charoensuksai P, Pichayakorn W. Characterization of antimicrobial agent loaded eudragit RS solvent exchange-induced *in situ* forming gels for periodontitis treatment. *AAPS Pharm Sci Technol* 2017;18:494–508.
- [25] Philippot P, Lenoir N, D'Hoore W, Bercy P. Improving patients' compliance with the treatment of periodontitis: a controlled study of behavioral intervention. *J Clin Periodontol* 2005;32:653–8.
- [26] Millan A, Bennema P, Verbeeck A, Bollen D. Morphology of silver bromide crystals from KBr-AgBr-DMSO-water systems. *J Cryst Growth* 1998;192:215–24.
- [27] Mura P. Analytical techniques for characterization of cyclodextrin complexes in the solid stage: a reviews. *J Pharm Biomed Anal* 2015;113:226–38.
- [28] Messner M, Kurkov SV, Jansook P, Loftsson T. Self-assembled cyclodextrin aggregates and nanoparticles. *Int J Pharm* 2010;387:199–208.
- [29] Szejtli J. *Cyclodextrin. Cyclodextrin technology*, 1. Netherlands: Springer; 1988. p. 1–78.
- [30] Katewongsa P, Lertsuphotvanit N, Phaechamud T. Cetirizine dihydrochloride/ $\beta$ -cyclodextrin inclusion complex by ethanol kneading for taste masking. *Indian J Pharm Sci* 2017:758–67.
- [31] Al-Marzouqi A, Jobe B, Dowaidar A, Maestrelli F, Mura P. Evaluation of supercritical fluid technology as preparative technique of benzocaine-cyclodextrin complexes-comparison with conventional methods. *J Pharm Biomed Anal* 2007;43:566–74.
- [32] Bettinetti GP, Mura P, Faucci MT, Sorrenti M, Setti M. Interaction of naproxen with non-crystalline acetyl- $\beta$ - and acetyl- $\gamma$ -cyclodextrins in the solid and liquid state. *Eur J Pharm Sci* 2002;15:21–9.
- [33] Hees TV, Piel G, de Hassonville H, Evrard B, Delattre L. Determination of the free/included piroxicam ratio in cyclodextrin complexes: comparison between UV spectrophotometry and differential scanning calorimetry. *Eur J Pharm Sci* 2002;15:347–53.
- [34] Lee DS, Hur P, Kim BK. Chemical hybridization of waterborne polyurethane with  $\beta$ -cyclodextrin by sol-gel reaction. *Prog Org Coat* 2017;111:101–11.
- [35] Giordano F, Novak C, Moyano JR. Thermal analysis of cyclodextrins and their inclusion compounds. *Thermochim Acta* 2001;380:123–51.
- [36] Chen M, Diao G, Zhang E. Study of inclusion complexes of  $\beta$ -cyclodextrin and nitrobenzene. *Chemosphere* 2006;63:522–9.
- [37] Xiong J, Jiang F, Zhou W, Liu C, Xu J. Highly electrical and thermoelectric properties of PEDOT:PSS thin-film via direct dilution-filtration. *RSC Adv* 2015;75:1–16.
- [38] Budavari S (ed). *The Merck index-an encyclopedia of chemicals, drugs and biological* Whitehouse Station, NJ: Merk and Co., Inc., 1996:p. 1378.
- [39] Bratu I, Hernanz A, Gavira JM, Bora GH. FTIR spectroscopy of inclusion complexes of  $\beta$ - cyclodextrin with fenbufen and ibuprofen. *Rom J Phys* 2004;50:1063–9.
- [40] Schalley CA. *Analytical methods in supramolecular chemistry*. Weinheim, Germany: Wiley-VCH Verlag GmbH & Co. KGaA; 2006. p. 817–54.
- [41] Catanescu O, Grigoras M, Colotin G, Dobreanu A, Hurduc N, Simionescu CI. Synthesis and characterization of some aliphatic-aromatic poly (Schiff bases). *Eur Polym J* 2001;37:2213–16.